Phonon properties and Raman response of (113) GaAs/AlAs corrugated superlattices

P. Castrillo,* G. Armelles, L. González, and P. S. Domínguez
Centro Nacional de Microelectrónica, Consejo Superior de Investigaciones Científicas, Serrano 144, 28006 Madrid, Spain

L. Colombo
Dipartimento di Fisica, Università di Milano, via Celoria 16, 20133 Milano, Italy
(Received 6 April 1994; revised manuscript received 27 September 1994)

We present an analysis of the vibrational properties and Raman response of (113)-oriented GaAs/AlAs superlattices with periodically corrugated interfaces. The vibrational properties have been calculated using the bond-charge model and the Raman response is evaluated in the framework of the bond polarizability model. We have measured the Raman spectra of samples grown by molecular-beam epitaxy, where an additional in-plane periodicity was expected, and of samples grown by atomic-layer molecular-beam epitaxy, which did not present this new in-plane periodicity. The comparison between the experimental results and the theoretical simulations suggests that faceting of the surface observed in the samples grown by molecular-beam epitaxy is not maintained in the buried interface.

I. INTRODUCTION

It has been recently proposed that (113)*A*-oriented (Al,Ga)As surfaces exhibit a spontaneous faceting so that an array of channels 10.2 Å high with a lateral periodicity of 32.0 Å is formed at high enough substrate temperatures.[1] In addition to this, it has been suggested that there is a phase change in the surface corrugation during the growth of GaAs on AlAs and AlAs on GaAs, which gives rise to the formation of quantum-wire-like (QWR) structures in GaAs/AlAs superlattices (SL's) [Fig. 1(c)]. Nevertheless, it has been recently shown[2] that some of the properties attributed to the existence of QWR-like structures are also observed in samples that did not present the proposed QWR-like structure. In this paper we address this problem using Raman spectroscopy, which has proved to be a very useful method to study the interface in GaAs/AlAs superlattices.[3] In the first part of the paper (Sec. II) we present the theoretical model used to calculate the vibrational properties of the SL with and without interface corrugation. We analyze the modification induced in the vibrational properties and Raman response by different types of interface corrugations and we show that Raman spectroscopy should be sensitive to detect the existence of the proposed lateral periodicity. In the second part of the paper (Sec. III) we compare the experimental results with the theoretical simulations. Finally, we discuss the information concerning the interface structure of the samples that is derived from the present study.

II. THEORY

The vibrational properties of the different SL's studied here are calculated using the bond-charge model.[4–6] In this work the same force constants, corresponding to GaAs, have been used for both GaAs and AlAs,[6] the dynamical difference between GaAs and AlAs being contained in the mass matrix. We focus our discussion on the GaAs-like phonons.

The dynamical matrix of the different SL's was calculated using a supercell approach described in Ref. 7. The different types of interfaces considered in this work are presented in Fig. 1. They correspond to sharp interfaces

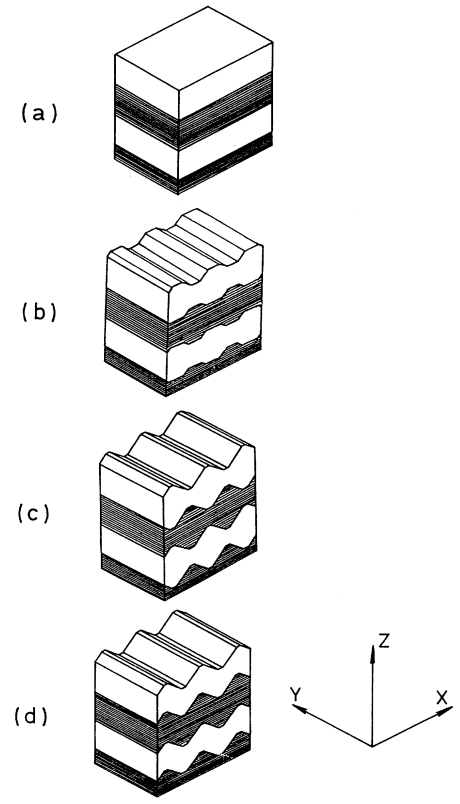

FIG. 1. Scheme of the different types of interfaces considered in this work: (a) sharp interfaces, (b) slightly corrugated interfaces, (c) quantum-wire-like structures, and (d) parallel corrugated interfaces. $\{\mathbf{x},\mathbf{yz}\}=\{[1\bar{1}0],[33\bar{2}]$, and $[113]\}$.

0163-1829/95/51(3)/1647(6)/$06.00

[panel (a)] and corrugated interfaces [panels (b)–(d)], with periodicity along the $[1\bar{1}0]$ direction. The corrugations presented in Fig. 1 have the same in-plane periodicity. The corrugation of Figs. 1(c) and 1(d) also have the same corrugation height. These types of corrugations have been chosen because they are, somehow, compatible with the experimental data presented as a proof of the existence of an interface of the type presented in Fig. 1(c) (see Ref. 1). This point will be discussed later in the paper.

We have performed calculations for SL's with GaAs layer thickness from 6 to 20 ML. For subsequent comparison with the experimental data (Sec. III), we will center our exposition around the theoretical results corresponding to a GaAs/AlAs SL with a GaAs layer thickness of 12 ML. We have verified that the calculated Raman spectra in the GaAs-related spectral range hardly depend on the thickness of the AlAs slab. The thickness of the AlAs slab has been chosen to be 12 ML, so that it is thick enough to confine the GaAs-related modes.

To calculate the Raman intensity we have used the bond-polarizability model (BPM).[8,9] We have taken from Ref. 9 the four parameters needed to describe the bond polarizability and their derivatives.

A. Noncorrugated superlattices

When compared with (001)-oriented GaAs/AlAs SL's, (113)-oriented GaAs/AlAs SL's present several peculiarities[9,10] that we present in the next paragraphs.

In (113)-oriented SL's the modes with **q** vector parallel to the growth axis have either pure transverse character (confined transverse-optical $TO_{[1\bar{1}0]}$ modes or propagating transverse-acoustic $TA_{[1\bar{1}0]}$ modes) or mixed transverse-longitudinal character (confined optical $TO_{[33\bar{2}]}$-$LO_{[113]}$ modes or propagating acoustic $TA_{[33\bar{2}]}$-$LA_{[113]}$ modes). Due to the mode mixing and to the low symmetry of the (113) plane, the envelope of the atomic displacement of the zone-center optical-confined modes is not as simple as for (001)-oriented SL's. Nevertheless, for layer thicknesses greater than 10 ML and for the first confined optical modes, the z patterns of the atomic displacements (LO character) have a sinusoidal-like form.

In Raman experiments and in the backscattering geometry the $TO_{[1\bar{1}0]}$ modes are only allowed in the $z(xy)\bar{z}$ configuration. The $LO_{[113]}$ and $TO_{[33\bar{2}]}$ modes are allowed in the $z(xx)\bar{z}$ and $z(yy)\bar{z}$ configurations, with x, y, and z the $[1\bar{1}0]$, $[33\bar{2}]$, and [113] directions, respectively.

B. Corrugated superlattices

1. Folding approximation

The existence of a periodicity in the growth plane superimposed to the existing one along the growth direction will influence the vibrational properties of the superlattices. We can argue that if the periodicity does not strongly affect the otherwise perfect interface, the vibrational properties of the system could be obtained from just a folding of the dispersion curve of the perfect SL along the direction of periodicity [folding approximation (FA)].[11]

In Fig. 2(a), we show the dispersion curve in the GaAs optical-phonon region of a $(GaAs)_{12}/(AlAs)_{12}$ SL along the $[1\bar{1}0]$ direction. The angular dispersion $\Gamma_{[113]}$-$\Gamma_{[1\bar{1}0]}$ is presented as well. The full points correspond to the frequencies of the first folded phonons assuming the lateral periodicity proposed in Ref. 1. As is shown in Fig. 2(b), the folded phonons have a strong mixed character. If the height of the corrugation is not negligible, the frequencies and displacements of the vibrational modes of a corrugated SL cannot be obtained from just a folding of the dispersion curve and a full calculation is needed.

2. Full calculation

In Fig. 3 we present the frequency position of the higher-frequency GaAs modes for a $(GaAs)_{12}/(AlAs)_{12}$ SL for the different types of corrugation shown in Fig. 1. In all the cases the lateral period is 32 Å but the height has been varied between 0 Å (sharp interfaces), 3.4 Å (2 ML), and 10.2 Å (6 ML). The displayed frequencies correspond to the modes originated at $\Gamma_{[113]}$. For the SL's with no corrugation, we have also displayed the frequencies of the modes coming from the folding of the branches along the $[1\bar{1}0]$ direction, which are twofold de-

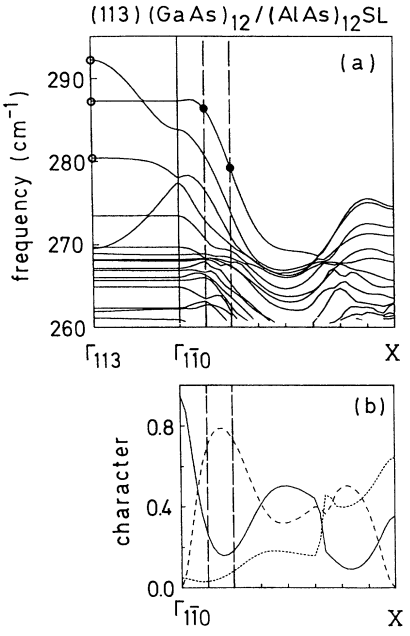

FIG. 2. (a) Phonon-dispersion curve along the $[1\bar{1}0]$ direction in the GaAs-like optical-phonon region for a $(GaAs)_{12}/(AlAs)_{12}$ (113)-oriented SL. The angular dispersion $\Gamma_{[113]}$-$\Gamma_{[1\bar{1}0]}$ curve is presented as well. The frequencies of the higher-frequency $\Gamma_{[113]}$ modes of the corrugated SL, obtained just by folding of the Brillouin zone, are indicated in the figure (circles, unfolded modes; dots, folded modes). (b) Phonon character plot for the first branch of the dispersion curve of (a); z character, solid line; y character, dotted line; x character, dashed line.

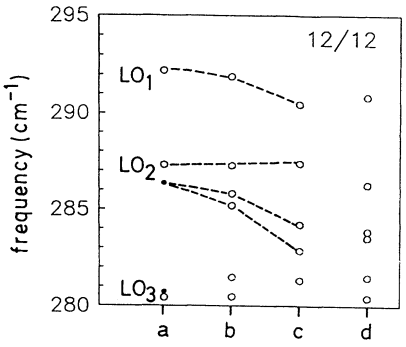

FIG. 3. Frequency of the $\Gamma_{[113]}$ modes of a $(GaAs)_{12}/(AlAs)_{12}$ SL for different degrees and types of interface corrugation. Only the frequency range 295–280 cm^{-1} is presented. *a*, sharp interfaces; *b*, interfaces of Fig. 1(b); *c*, interfaces of Fig. 1(c); *d*, interfaces of Fig. 1(d). For sharp interfaces, we have also displayed the frequency of the modes obtained just by folding the Brillouin zone (dots) (see Fig. 2). The unfolded longitudinal-optical modes are labeled by LO_n. The dashed lines are a guide for the eye.

generate. In this way, we can compare the results of the full calculation for the corrugated structures with the results of the FA. The frequency of the first confined phonon (LO_1) decreases as we increase the corrugation. The behavior of the other LO modes (LO_2,LO_3, . . . ,) is, in general, more complicated due to the interaction between the different modes. Moreover, we can observe the splitting of the twofold degenerate folded modes.

In Fig. 4, we present the displacement patterns of the first four phonons confined in the GaAs layers of the QWR-like SL [structure of Fig. 1(c)] and we compare them with the displacements patterns obtained using the FA. For the unfolded modes [LO_1 and LO_2, shown in panels (c1) and (c2), respectively] we can observe a lateral modulation of the amplitude. The second mode, which has mainly a z component, is localized in the GaAs channels and has also a strong x component. We would like to emphasize the appearance of the u_x component in all the displacement patterns of the modes in the corrugated SL's. The effects of the corrugation decrease when the corrugation intensity decreases.

The different components of the displacement patterns (u_x, u_y, u_z) have well-defined parity along the [1$\bar{1}$0] direction (x axis). The parity of the u_x pattern has opposite sign than the parity of the u_y and u_z patterns. The modes whose u_x pattern has odd parity along the x axis [modes (c1), (c2), and (c4) of Fig. 4] have vanishing intensity in the $z(xy)\bar{z}$ configuration, while the modes with odd parity in the u_y and u_z patterns [mode (c3) of Fig. 4] have vanishing intensity in the $z(xx)\bar{z}$ and $z(yy)\bar{z}$ configurations.

Figure 5 shows the theoretical Raman response in the backscattering configuration of a $(GaAs)_{12}/(AlAs)_{12}$ SL with two types of corrugations. The Raman response of a noncorrugated SL (dashed lines) is shown as well. For these simulations we assumed Lorentzian line shapes with a broadening parameter of 1 cm^{-1}. The significative phonons of the noncorrugated SL have been labeled according to their dominant character and to their confinement order. A simple assignation is not possible for most of the phonons of the corrugated SL's, due to their strongly mixed character.

The most remarkable effects of the corrugation are the decrease of the LO_1 phonon frequency and the appearance of peaks in the $z(xy)\bar{z}$ spectra at frequencies higher than the $TO_{1\bar{1}0}$ branch of bulk material. These peaks have a strong x component ($TO_{1\bar{1}0}$ character) but also y and z components, they are different for the different types of corrugation, and do not appear in the case of noncorrugated SL's. Therefore, the $z(xy)\bar{z}$ Raman response can be used to characterize the existence and type of interface corrugation.

As expected, the calculated differences between the Raman spectra for corrugated and flat SL's are smaller for thicker SL's, but they should still be distinguishable for a SL with GaAs layer thickness up to 20 ML.

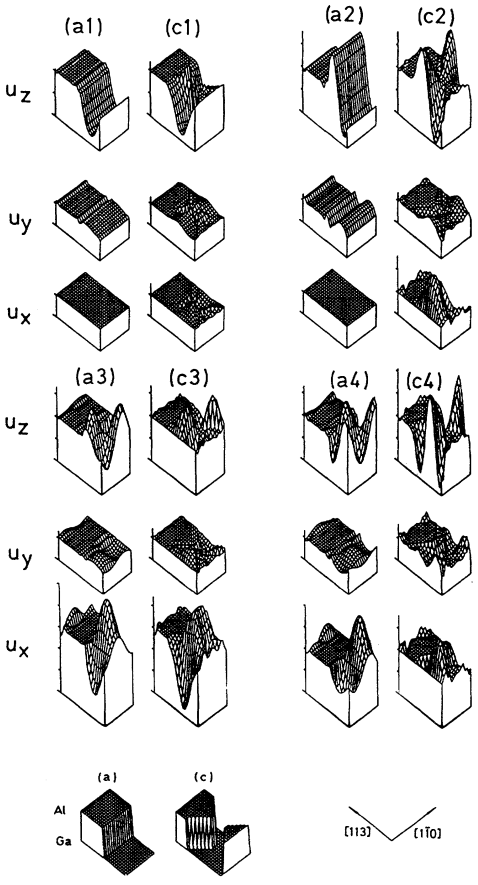

FIG. 4. Envelope of the different components (u_x, u_y, and u_z) of the cationic displacement **u** for the first four phonons of a $(GaAs)_{12}/(AlAs)_{12}$ SL with lateral periodicity along the [1$\bar{1}$0] direction. (a1): sharp interfaces (ω_{a1}=292.2 cm^{-1}, ω_{a2}=287.3 cm^{-1}, $\omega_{a3}=\omega_{a4}$=286.3 cm^{-1}). (c1) Corrugated interface of the type of Fig. 1(c) ω_{c1}=290.4 cm^{-1}, ω_{c2}=287.4 cm^{-1}, ω_{c3}=284.8 cm^{-1}, ω_{c4}=282.2 cm^{-1}). x, [1$\bar{1}$0]; y, [33$\bar{2}$]; and z, [113].

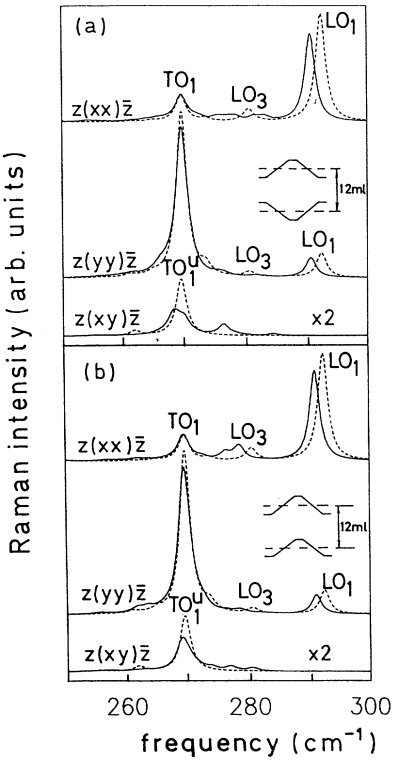

FIG. 5. Theoretical Raman spectra of a $(GaAs)_{12}/(AlAs)_{12}$ SL with (a) corrugated interfaces of the type of Fig. 1(c) and (b) corrugated interfaces of the type of Fig. 1(d). The Raman spectra of the same SL with flat interfaces is also shown (dashed line). The labels of the peaks correspond to the SL with flat interfaces (see text).

III. EXPERIMENTAL RESULTS AND DISCUSSION

The samples used in this work were grown by molecular-beam epitaxy (MBE) and atomic-layer molecular-beam epitaxy[12] (ALMBE) on (113)A GaAs substrates. During the growth by ALMBE, carried out at low substrate temperatures (typically 375 °C), the characteristic splitting along the streaks of the reflection high-energy electron-diffraction (RHEED) pattern, which is an indication of the additional in-plane periodicity of the SL,[1] was not observed. Such RHEED pattern features, however, were distinctly observed when growth took place by MBE. The structural parameters of the samples as determined by x-ray diffraction are $(GaAs)_{14}/(AlAs)_{47}$ and $(GaAs)_{20}/(AlAs)_{50}$ for the samples grown by ALMBE (which we labeled $A1$ and $A2$, respectively), and $(GaAs)_{12}/(AlAs)_{55}$ and $(GaAs)_{17}/(AlAs)_{50}$ for the MBE samples (which we labeled $B1$ and $B2$, respectively). The Raman spectra were recorded at 80 K in a backscattering geometry using a SPEX triplemate spectrograph equipped with a charge-coupled-device camera.

Next, we discuss the spectra for the samples with thinner GaAs layers (samples $A1$ and $B1$) in which, according to the theoretical results, the modifications induced by the corrugation should be stronger.

In Fig. 6 we present the experimental Raman spectra in the GaAs phonon range corresponding to samples $A1$ and $B1$. These SL's have quite similar thickness for the GaAs slab and were grown by ALMBE and MBE, respectively. The spectra of Fig. 6 were obtained by exciting with the 488.0-nm line of an Ar^+ laser and correspond to off-resonance conditions. Therefore, they can be compared with the Raman intensities calculated with the BPM. In both cases, no extra peaks are observed in the $z(xy)\bar{z}$ spectrum above the frequency of the $TO_{[1\bar{1}0]}$ branch, contrary to the predictions for the QWR-like corrugated SL's. Moreover, for both cases, the frequency of the first longitudinal phonon (LO_1) agrees with the calculation assuming sharp interfaces. Consequently, the experimental peaks in both Figs. 6(a) and 6(b) have been labeled according to the calculation for a SL with sharp interfaces. TO_1^u refers to the first confined $TO_{[1\bar{1}0]}$ mode

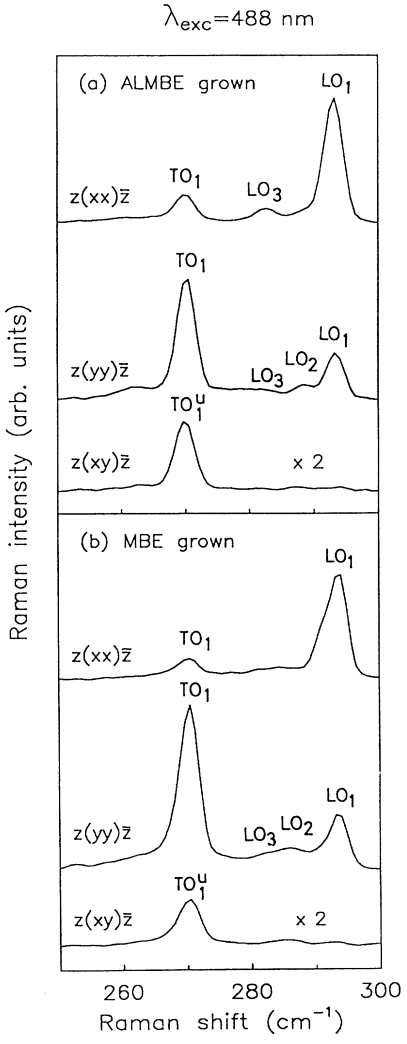

FIG. 6. Experimental Raman spectra taken in the backscattering geometry at 80 K using the 488-nm line of an Ar^+ laser. (a) sample $A1$; (b) sample $B1$. The labels of the peaks correspond to the predominant character of the phonons.

and TO_1 refers to the first mainly $TO_{[33\bar{2}]}$ confined mode. The LO_2 phonon, resolved in the $z(yy)\bar{z}$ spectrum, has no negligible Raman intensity due to some small contribution of the Frölich interaction. This assignment is consistent with the resonant behavior that we have observed when we have excited with other laser lines lying closer to the relevant electronic transitions.

Sample $B1$ has the same thickness for the GaAs slab as the one considered in the calculations. However, the experimental spectra of this sample are very different from the simulations for the corrugated SL's shown in Fig. 5. In fact, the experimental spectra are more similar to those of a noncorrugated SL. The only significant difference between the spectra of the two samples shown in Fig. 6 is the more pronounced broadening of the LO_3 peak in sample $B1$ [see the $z(xx)\bar{z}$ spectra]. This can be attributed to the different degree of interface roughness,[3] without invoking the existence of periodic faceting. No evidence of interface corrugation is obtained from the study of the other samples ($A2$ and $B2$).

Other experimental results for (113)A-oriented GaAs/AlAs SL's have been recently reported.[10,13] The Raman spectra presented there correspond to $(GaAs)_{14}/(AlAs)_{13}$ and $(GaAs)_{17}/(AlAs)_{17}$ SL's, grown under conditions identical to those proposed for the generation of QWR-like structures. The spectra recorded under off-resonance conditions, shown in Ref. 10, are similar to our spectra. They agree with the simulations assuming flat interfaces and are rather different from the simulated spectra for 14/13 and 17/17 SL's with periodically corrugated interfaces. Additionally, we would like to point out that an overall understanding of the phonon properties of these SL's has been achieved on the basis of theoretical models assuming flat interfaces.[10,13]

From the analysis of the experimental data and from the comparison with the ALMBE-grown samples, it is very clear that the Raman spectra of MBE-grown SL's do not correspond with the Raman response of the proposed QWR-like structure. Very recent scanning-tunneling-microscope images taken on a GaAs (113)A surface exhibit the same lateral periodicity as the one derived from the RHEED patterns (32 Å).[14] However, the height of the corrugation is only 3.4 Å (2 ML), and thus much smaller than that of the previously proposed model. So far, it is not clear if this surface corrugation remains stable at the GaAs/AlAs interface during the growth of the SL's. For the samples studied here, Raman spectroscopy is not sensitive enough to exclude the existence of a remaining interface corrugation (1 or 2 ML high).

In an early paper,[11] resonant Raman spectra have been reported for (113)A-oriented GaAs/AlAs SL's. Additional peaks were observed in the spectral range of the GaAs-confined modes and were attributed to folded modes related to the lateral periodicity. As these data are related to the lateral period of the corrugation but not directly to its height, the observed peaks might come from a weakly corrugated structure under particular conditions of resonant excitation. We have also explored the hypothesis that the additional peaks of Ref. 11 could have an origin different from any lateral periodicity. In particular, we have verified the possibility that these peaks could be related with the so-called "interfacelike phonons" (having $q \sim 0$ and $\mathbf{q}$ perpendicular to z), which have a more complicated phenomenology for the SL's grown along low-symmetry directions than for the standard (001)-oriented SL's.[9,10,15] These modes, not allowed in backscattering configuration, can be activated under resonant conditions. The agreement between the calculated frequencies for these modes and the frequencies of the experimental peaks supports this possibility.

IV. CONCLUSIONS

In conclusion, we have analyzed the influence of interface corrugation on the vibrational properties of (113) GaAs/AlAs SL's. The most important effects on the Raman response are (i) the appearance of peaks at frequencies higher than the $TO_{[1\bar{1}0]}$ branch in the $z(xy)\bar{z}$ Raman spectra of the corrugated SL's, which are not present in the noncorrugated SL's, and (ii) the shift of the LO_1 peak to lower frequencies. We have measured the Raman spectra of samples grown both by ALMBE and MBE techniques. The splitting of the RHEED pattern, characteristic of the in-plane periodicity, was only observed in MBE samples. The Raman spectra of the samples grown by MBE or ALMBE are similar and we have not observed the effects of the proposed interface corrugation. These results suggest that if the surface corrugation has a counterpart in the buried interface, this effect is weak or not very reproducible.

ACKNOWLEDGMENTS

This work has been partially supported by the Spanish Comisión Interministerial de Ciencia y Tecnología under Project No. MAT92-0262. One of us (L.C.) acknowledges financial support from the Italian Consiglio Nazionale delle Ricerche through the "Progetto Finalizzato Materiali Speciali per Tecnologie Avanzate."

*Present address: Departamento de Electricidad y Electrónica, Universidad de Valladolid, Prado de la Magdalena, s/n 47005 Valladolid, Spain.

[1] R. Nötzel, N. N. Ledentsov, L. Däweritz, M. Hohenstein, and K. Ploog, Phys. Rev. Lett. **67**, 3812 (1991); R. Nötzel, N. N. Ledentsov, L. Däweritz, K. Ploog, and M. Hohenstein, Phys. Rev. B **45**, 3507 (1992).

[2] G. Armelles, P. Castrillo, P. S. Domínguez, L. González, A. Ruiz, D. A. Contreras-Solorio, V. R. Velasco, and F. García-Moliner, Phys. Rev. B **49**, 14 020 (1994).

[3] B. Jusserand, F. Alexandre, D. Paquet, and G. Le Roux, Appl. Phys. Lett. **47**, 301 (1985); B. Jusserand, F. Mollot, J. M. Moisson, and G. Le Roux, *ibid.* **57**, 560 (1990).

[4] W. Weber, Phys. Rev. B **15**, 4789 (1977); K. C. Rustagi and W. Weber, Solid State Commun. **18**, 673 (1976).

[5] L. Miglio and L. Colombo, Surf. Sci. **221**, 486 (1989).

[6] M. Bernasconi, L. Colombo, L. Miglio, and G. Benedek, Phys. Rev. B **43**, 14 447 (1991); **43**, 14 457 (1991).

[7] L. Miglio and L. Colombo, Superlatt. Microstruct. **7**, 139 (1990).

[8]B. Jusserand and M. Cardona, in *Light Scattering in Solids V*, edited by M. Cardona and G. Güntherodt (Springer-Verlag, Heidelberg, 1989), p. 91, and references therein.
[9]P. Castrillo, L. Colombo, and G. Armelles, Phys. Rev. B **49**, 10 362 (1994).
[10]Z. V. Popovic, E. Richter, J. Spitzer, M. Cardona, A. J. Shields, R. Nötzel, and K. Ploog, Phys. Rev. B **49**, 7577 (1994).
[11]A. J. Shields, R. Nötzel, M. Cardona, L. Däweritz, and K. Ploog, Appl. Phys. Lett. **60**, 2537 (1992).
[12]F. Briones, L. González, and A. Ruiz, Appl. Phys. A **49**, 729 (1989).
[13]A. J. Shields, Z. V. Popovic, M. Cardona, J. Spitzer, R. Nötzel, and K. Ploog, Phys. Rev. B **49**, 7584 (1994).
[14]M. Wassermeier, J. Sudijono, M. D. Johnson, K. T. Leung, B. G. Orr, L. Däweritz, and K. Ploog (unpublished).
[15]Z. V. Popovic, M. Cardona, E. Richter, D. Strauch, L. Tapfer, and K. Ploog, Phys. Rev. B **43**, 4925 (1991).